

SCIENTIFIC REPORTS



OPEN

Umbilical cord-derived mesenchymal stem cell extracts ameliorate atopic dermatitis in mice by reducing the T cell responses

Ji-young Song¹, Hyo Jeong Kang², Hyun Min Ju¹, Arum Park¹, Hyojung Park¹, Joon Seok Hong³, Chong Jai Kim², Jae-Yoon Shim⁴, Jinho Yu⁵ & Jene Choi²

Mesenchymal stem cells derived from Wharton's jelly of the umbilical cord (UC-MSCs) have immunomodulatory properties. The aim of this study was to explore whether extracts of MSCs (MSC-Ex) could augment the low therapeutic efficacy of the whole cells in an *Aspergillus fumigatus* (Af)-induced atopic dermatitis (AD) model. LPS- or TNF- α /IFN- γ -stimulated keratinocytes (HaCaT cells) were treated with MSC-Ex, and the Af-induced AD model was established in BALB/c mice. In HaCaT cells, MSC-Ex treatment significantly reduced the inflammatory cytokine (IL-6, IL-1 β , IL-4, IL-5 and TNF- α), iNOS and NF- κ B levels, and upregulated the anti-inflammatory cytokines (IL-10 and TGF- β 1). In the AD mice, the MSC-Ex group showed greatly reduced dermatitis, and lower clinical symptom scores and IgE levels. The histological dermatitis scores were also markedly lower in the MSC-Ex-treated animals compared with the MSC-treated group. Decreased levels of IFN- γ (Th1) and IL-17 (Th17), IL-4 and IL-13 (Th2) were detected in T cells and the skin tissue from the MSC-Ex treated AD mice. The therapeutic capacity of MSC-Ex was preserved after lyophilization and reconstitution. MSC-Ex treatment reproducibly suppresses dermatitis and inhibits the induction of inflammatory cytokines in the skin of AD mice. MSC-Ex is therefore a potential new treatment agent for AD.

Atopic dermatitis (AD) is a chronic inflammatory dermatopathy that features eczematous skin lesions with severe pruritus and affects up to 20% of children and 10% of adults^{1,2}. The pathogenesis of AD is characterized by dominant type 2 helper T cell (Th2)-mediated abnormal inflammatory responses, resulting in B lymphocyte-mediated increases in serum immunoglobulin E (IgE)³⁻⁵. Subsequent degranulation of mast cells by the elevated IgE releases and recruits lymphocytes and eosinophils to the AD lesion. The current clinical management of AD comprises topical corticosteroids and systemic immunosuppressive agents^{5,6}. However, the long-term use of these drugs is associated with a series of well-documented side effects, including growth disturbance, osteoporosis, cataracts, and the development of lymphopenia⁷⁻⁹.

Several recent studies have indicated that the use of mesenchymal stem cells (MSCs) is a promising therapeutic approach for AD. Shin and colleagues reported that intravenously injected human adipose tissue-derived MSCs (AT-MSCs) alleviate AD by suppressing B lymphocyte proliferation and maturation via COX-2 signaling¹⁰. Moreover, subcutaneously injected human umbilical cord blood-derived MSCs (UCB-MSCs) have shown a dose-dependent clinical efficacy in moderate-to-severe adult AD patients in a clinical trial (phase I/IIa); about 58% of the patients in the trial exhibited a 50% reduction in the Eczema Area and Severity Index score¹¹.

¹Institute for Life Science, University of Ulsan College of Medicine, Asan Medical Center, Seoul, Korea. ²Department of Pathology, University of Ulsan College of Medicine, Asan Medical Center, Seoul, Korea. ³Department of Obstetrics and Gynecology, Seoul National University Bundang Hospital, Gyeonggi-do, Korea. ⁴Department of Obstetrics and Gynecology, University of Ulsan College of Medicine, Seoul, Korea. ⁵Department of Pediatrics, Asan Medical Center, University of Ulsan College of Medicine, Seoul, Korea. Correspondence and requests for materials should be addressed to J.Y. (email: jinhoyu@amc.seoul.kr) or J.C. (email: jene@amc.seoul.kr)

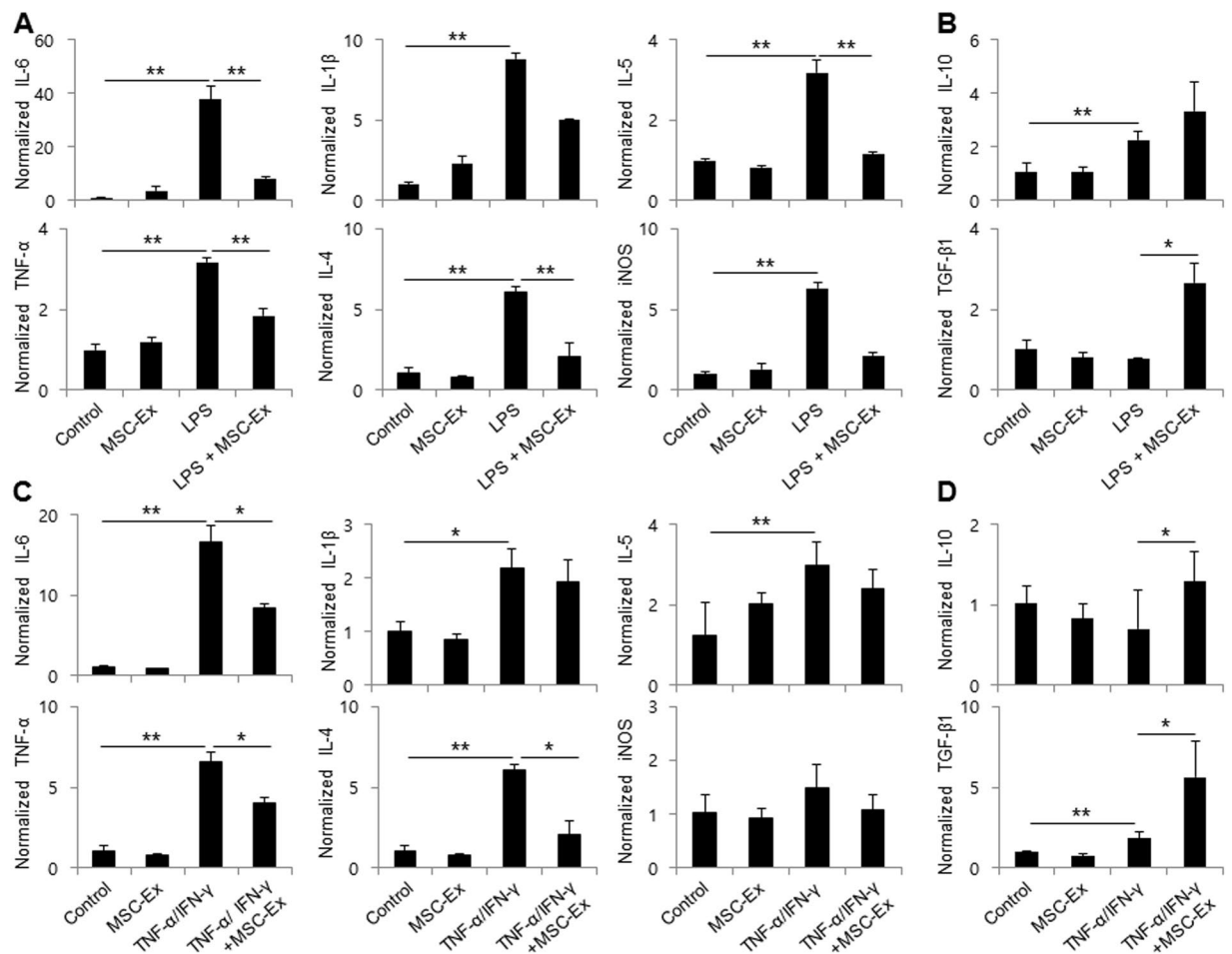


Figure 1. MSC-Ex decreases the expression of pro-inflammatory cytokines in LPS- or TNF- α /IFN- γ -stimulated HaCaT cells. The relative expression levels of the inflammatory-associated genes were evaluated by qRT-PCR after stimulation by LPS for 4 h (100 μ g/ml) or TNF- α /IFN- γ (10 ng/ml each) for 2 h and then subsequently after MSC-Ex (30 μ g/ml) treatment for 24 h with LPS: IL-6, TNF- α , IL-1 β , IL-4, IL-5 and iNOS (A,C), IL-10 and TGF- β 1 (B,D). Columns represent the means of three independent experiments; bars indicate standard deviations. * $P < 0.05$, ** $P < 0.005$, *** $P < 0.001$.

Human umbilical cord-MSCs (UC-MSCs) are obtained from the Wharton's jelly of the umbilical cord and are distinguishable from the MSCs present in UC blood (UCB-MSCs)^{12,13}. UC-MSCs have been most widely used for the treatment of various inflammatory diseases because they can be easily isolated in large quantities from postnatal cord tissues^{14,15} and express low levels of type I HLA antigen, but do not express type II HLA antigens or T cell co-activators¹⁶. Many prior studies have reported that only a limited number of engrafted MSCs reach inflamed damaged tissues and are rapidly cleared post-administration^{10,17}. In our current study, we investigated the therapeutic effects of UC-MSC extracts (MSC-Ex) in an *Aspergillus fumigatus* (*Af*)-induced AD mouse model. Treatment with MSC-Ex efficiently blocked the induction of pro-inflammatory cytokines and reduced both atopic histopathological symptoms and immune responses in these animals. The clinical therapeutic effects of MSC-Ex were thus found to be superior to that of MSCs.

Results

MSC-Ex suppresses pro-inflammatory cytokines in keratinocytes. HaCaT cells were stimulated with LPS (100 μ g/ml) for 28 h to investigate whether MSC-Ex treatment generated anti-inflammatory effects in human keratinocytes. As expected, LPS increased the mRNA levels of the proinflammatory cytokines IL-6, IL-1 β , and TNF- α , as well as those of the Th2 cytokines IL-4 and IL-5. MSC-Ex treatment significantly decreased the mRNA levels of these five cytokines and suppressed the expression of inducible NO synthase (iNOS) in LPS-stimulated HaCaT cells ($P < 0.01$). In contrast, MSC-Ex treatment increased the mRNA levels of the anti-inflammatory cytokines IL-10 and TGF- β 1 ($P < 0.05$) (Fig. 1A,B). MSC-Ex suppressed the expression of the above-mentioned Th1- and Th2-type cytokines after stimulation with TNF- α and IFN- γ (Fig. 1C,D). These data indicate that MSC-Ex suppresses the Th1 and Th2 inflammatory responses of human keratinocytes.

MSC-Ex inhibits NF- κ B activity. NF- κ B plays a key role in regulating the immune response to inflammatory diseases. PPAR α inhibits NF- κ B-dependent transcriptional activation and subsequent inflammatory

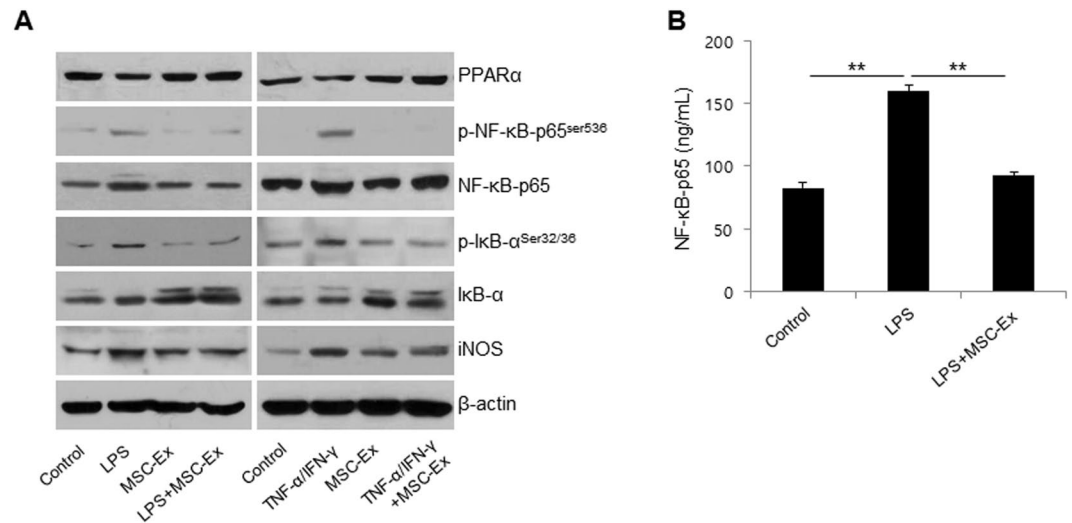


Figure 2. MSC-Ex restores the PPAR α activity in HaCaT cells. **(A)** HaCaT cells were treated as described in Fig. 1 and western blot analyses were performed using primary antibodies for PPAR α , NF- κ B-65, p-NF- κ B-p65^{Ser536}, I κ B, p-I κ B^{Ser32/36} and iNOS. β -Actin was used as the loading control. **(B)** The protein levels of NF- κ B were determined by ELISA. Columns represent the means of three independent experiments; bars indicate standard deviations. $*P < 0.05$, $**P < 0.005$, $***P < 0.001$.

responses^{18,19}. To further examine the mechanisms underlying the reduction in inflammatory responses by MSC-Ex, we assayed NF- κ B and PPAR α in LPS- or TNF- α and IFN- γ -stimulated HaCaT cells (Fig. 2A). MSC-Ex significantly reduced the NF- κ B and iNOS protein and inversely increased PPAR α and I κ B, the inhibitor of NF- κ B. In addition, the MSC-Ex-treated cells exhibited low levels of p-I κ B- α at Ser32/36 and p-NF- κ B at Ser536, which are required for the transactivating function of NF- κ B, compared with the stimulated control. The NF- κ B protein levels following MSC-Ex treatment were confirmed by ELISA ($P < 0.01$) (Fig. 2B). These data supported that the immune mediator NF- κ B is strongly antagonized by MSC-Ex in inflammatory keratinocytes.

MSC-Ex ameliorates *Aspergillus fumigatus* (Af)-induced AD. We hypothesized that a robust administration of paracrine factors using MSC-Ex may be a viable alternative to UC-MSCs in the treatment of AD as it would overcome the low survival rate of the whole cells *in vivo*. An *Af*-induced AD mouse model was used to investigate the therapeutic effects of MSC-Ex *in vivo*. UC-MSCs (2×10^6 cells/mouse) and MSC-Ex (300 μ g) prepared from an identical number of MSCs were administered subcutaneously to the AD mice on day 23 (Fig. 3A). Both treatments significantly reduced the clinical scores after 5 days. Compared to the MSC-Ex treatment, however, UM-MSCs showed a trend towards a stronger reduction of the clinical symptom scores (Fig. 3B). UC-MSC and MSC-Ex treatments both reduced the TEWL and IgE levels in the serum to a comparable degree (Fig. 3C,D). Taken together, these data indicated that UC-MSC and MSC-Ex have a similar therapeutic efficacy against AD that may result from the systemic regulation of allergic responses.

MSC-Ex has a superior therapeutic efficacy to UC-MSCs in the AD mouse model. We assessed the severity of AD histologically in the mouse model using a scoring system for hyperkeratosis, parakeratosis, psoriasisiform epidermal hyperplasia, hypergranulosis, and prominent or absent spongiosis. The MSC-Ex treated group showed significantly improved dermatitis parameters such as lower hypergranulosis and psoriasisiform epidermal hyperplasia compared with the animals who received MSCs (Fig. 4A). However, we did not detect differences in the depth of fibrosis between the MSC-Ex-treated and the MSC treated groups (Fig. 4B). Collectively, our findings indicated greatly decreased total histological dermatitis scores in the MSC-Ex treated group (Fig. 4C) and that MSC-Ex had markedly superior therapeutic efficacy to MSCs in the AD mouse model (mean of total score, 6.0 vs 4.2).

MSC-Ex suppresses T cell activation. The pathogenesis of AD is defined by an imbalance in Th1, Th2, Th17, and Treg cells²⁰. To further investigate T cell differentiation in our AD mice, the levels of IFN- γ (Th1), IL-17 (Th17), IL-4 (Th2) and IL-10 (Th9) were measured in anti-CD3/CD28 activated T cells derived from the local LNs of the UC-MSC- or MSC-Ex-treated animals. The levels of the pro-inflammatory cytokines IFN- γ and IL-17 were significantly decreased in T cells in the MSC-Ex-treated group compared to the untreated control and UC-MSC-treated groups. Moreover, MSC-Ex treatment resulted in levels of IL-4 and IL-10 similar to those of the healthy control group (Fig. 5A). Next, we examined the expression levels of pro-inflammatory cytokines in the skin tissue of AD mice. The expression levels of the pro-inflammatory cytokines TNF- α , IFN- γ , IL-17, and IL-13 were decreased (Fig. 5B), and immunoblotting showed (Fig. 5C) that the activation pattern of the NF- κ B pathway was identical to that in HaCaT cells (Fig. 2A). Hence, MSC-Ex promotes immunosuppressive and suppresses T cell activation, and shows a higher therapeutic efficiency than the whole cells.

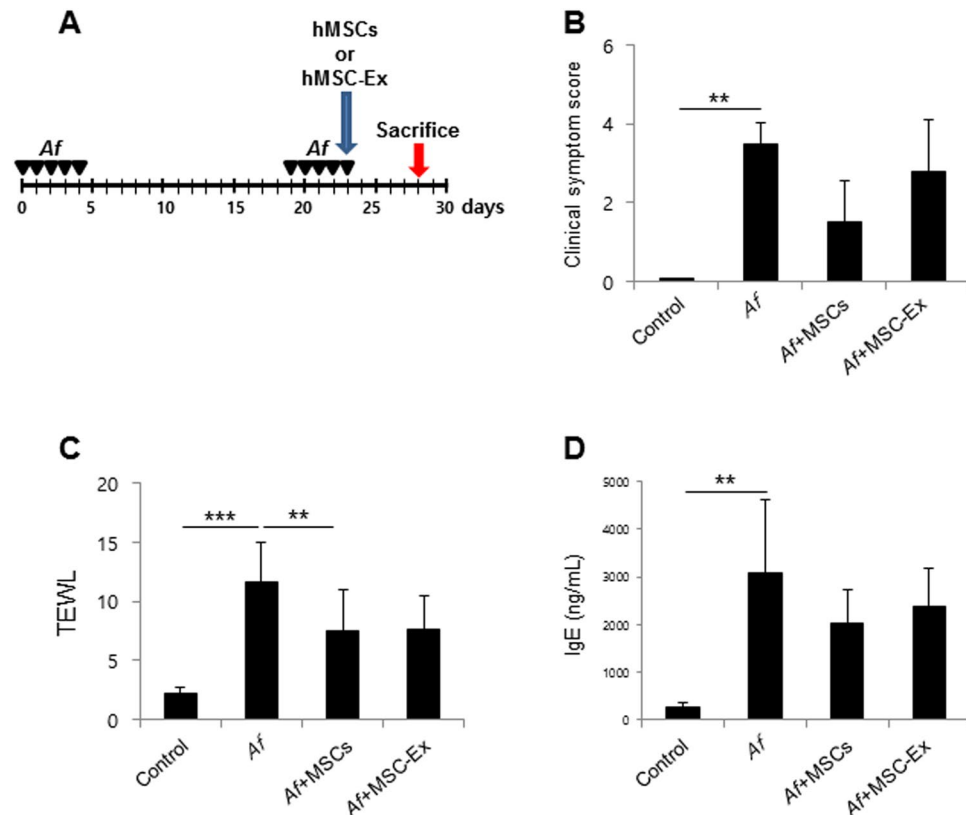


Figure 3. MSC-Ex treatment attenuates AD in the *Af*-induced mouse model. (A) Schematic protocol for *Af*-induced mouse AD and s.c. injection of MSCs (2×10^6 cells) or MSC-Ex (300 μ g), respectively. (B) Clinical symptom scores were calculated on the last day of the experiment (day 28) based on the clinical Psoriasis Area and Severity Index. (C) TEWL in the mouse dorsal skin was measured at the end of the experiment. (D) The IgE levels in serum were measured using ELISA. Data are represented as the means \pm s.d. ($n \geq 6$ mice per group). * $P < 0.05$, ** $P < 0.005$, *** $P < 0.001$.

The therapeutic capacity of MSC-Ex is preserved after lyophilization. MSC-Ex would have to show product stability to be developed as a future therapeutic agent. We examined whether the stability and performance of MSC-Ex would be preserved after lyophilization. MSC-Ex powder was reconstituted in PBS after 5 days of freeze drying and then administered to LPS-stimulated RAW 264.7 macrophage cells. In the co-cultured RAW 264.7 cells, reconstituted MSC-Ex (MSC-Ex-R) significantly reduced the levels of nitrite, a principal final metabolite of NOS and an inflammation marker. The therapeutic efficiency of this preparation was comparable with that of the original MSC-Ex (Fig. 5D). These data further support the potential for MSC-Ex to be used as a cell-free treatment for AD.

Discussion

MSC therapy has emerged as a promising strategy for a range of immune-mediated conditions and previous studies have reported encouraging results with these cells in inflammatory diseases. However, the clinical outcomes of these treatments with respect to efficiency are variable, likely due to the heterogeneity resulting from the use of bone marrow-, adipose-, UC blood-, or UC (Wharton's jelly)-derived MSCs, the homing efficiency of MSCs, and the different microenvironments that the engrafted cells have encountered in different studies. In our current study using an AD mouse model, we tested the proposition that umbilical cord-derived MSC extracts (MSC-Ex) would be as safe but have superior efficacy to MSCs by analyzing their paracrine effects. Our results indicated that subcutaneously injected MSC-Ex significantly improves the inflammatory symptoms in *Af*-induced AD mice and shows no loss of potency after freeze drying and reconstitution in buffer.

One of the ongoing debates in stem cell therapy is the homing efficiency of engrafted MSCs to a site of injury or inflammatory sites. In some preclinical disease models, the infused stem cells have been found to be entrapped mainly in other organs such as the liver and lungs¹⁷. Recently, Shin and colleagues reported that the majority of MSCs are detected in the lung and heart in a murine AD model after intravenous injection¹⁰. Our present *in vitro* and *in vivo* data provide evidence that robust administration of anti-inflammatory paracrine factors contained in the MSC-Ex preparation inhibited T-cell-driven inflammatory responses via reductions in the levels of IFN- γ (Th1 cell marker), IL-17 (Th17 cell marker), IL-4, IL-5 and IL-13 (Th2 cell marker) and B-cell-mediated serum IgE (Figs 1, 3 and 5), which were reported in chronic colitis models¹⁵. These results further indicate that MSC-Ex attenuates allergic responses systemically and has an efficacy via a one-time injection that is comparable to the equivalent number of injected and entrapped MSCs that secrete anti-inflammatory cytokines over 5 days (Fig. 3).

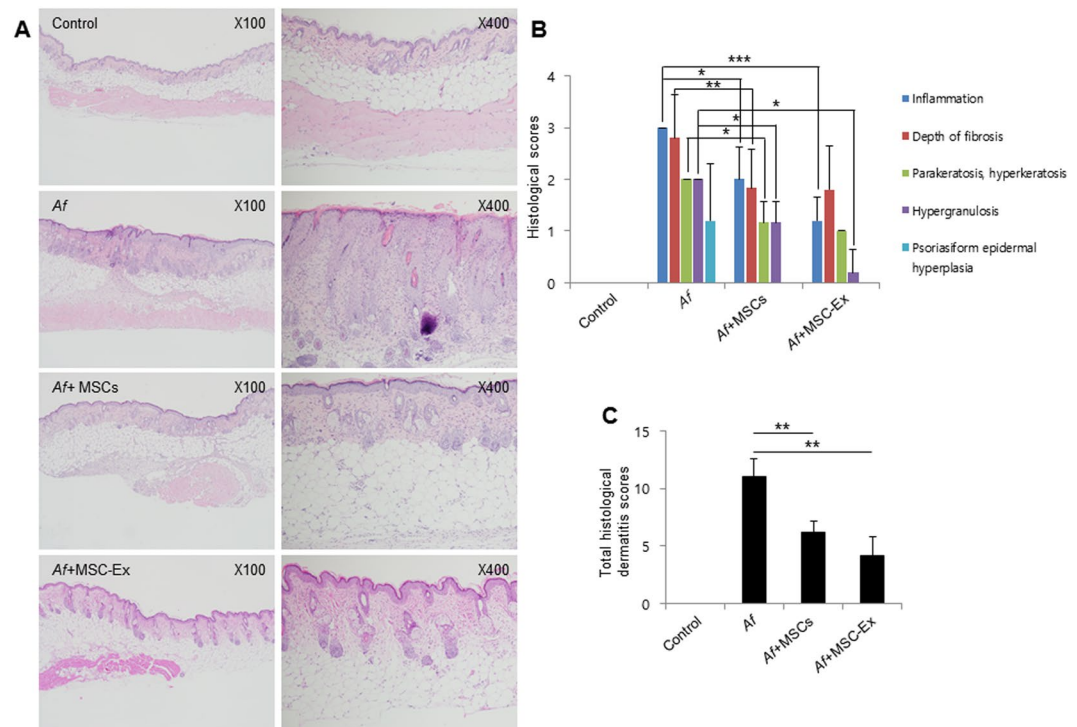


Figure 4. MSC-Ex reduces dermatitis in the AD mouse model. (A) Macroscopic appearance of the skin sections of the dorsal surface (original magnification, 100x and 400x). (B) Histological symptoms of AD used to assess disease severity by histology. (C) Total histological AD scores were determined. Data are represented as the means \pm s.d. ($n \geq 6$ mice per group). * $P < 0.05$, ** $P < 0.005$, *** $P < 0.001$.

The toxicity of MSCs has been evaluated previously by testing various dose levels. Establishing a single cell dose limit will be ideal for future applications of these cells in clinical therapy. We here injected 2×10^6 UC-MSCs per mouse or MSC-Ex prepared from this same number of cells (equaling 300 μ g per mouse). These dosage levels did not cause any adverse events or abnormal inflammatory responses at the injected sites.

A number of studies have reported that MSCs secrete soluble factors, but that they become undetectable only a few days after injection^{15,21,22}. The most interesting point in this regard is that the therapeutic effects of MSCs seem to be dependent on the specific microenvironment that the cells encounter after their injection²³. Polchert *et al.* have reported that bone marrow-isolated MSCs are effective at day 2 and 20, but not at day 0 and 30 in a graft *versus* host disease (GVHD) mouse model²⁴. Toll-like receptor 3/4 (TLR3/4)-activated MSCs promote inflammatory responses via the production of inflammatory mediators such as IL-1 β , IL-6, IL-8/CXCL8, and CCL5 against pathogens²⁵. The contradictory or even opposite outcomes of inflammatory disease models and clinical studies could be due to different cytokine concentrations and differences in the cross talk between MSCs and the local microenvironment. Our current results in the mouse show that MSC-Ex ameliorates the clinical symptoms of AD (dryness, scaling, erosion, excoriation, and hemorrhage) as well as reduces the TEWL and IgE levels, but we found a lower local immunologic response level at the site of MSC-Ex injection compared with that of MSC injection (unpublished data).

Of note, we found that the levels of IL-17 and IFN- γ were greatly reduced in T cells from the MSC-Ex-treated group compared with the MSC-treated group (Fig. 5A). The percentage of Th17 cells was significantly correlated with that of IFN- γ -producing Th1 cells in the peripheral blood of patients with AD and was associated with AD severity²⁶. Thus, we contend that MSC-Ex modulates IL-17-secreting Th17 as well as Th1/Th2 cells such that the physiological conditions are shifted from pro-inflammatory to anti-inflammatory. Therefore, MSC-Ex immediately interferes with both the innate and adaptive immune systems, rather than slowly reprogramming the immune cells via cell-to-cell interactions in host tissues, as MSCs play a role. We utilized *Aspergillus fumigatus*, a fungal pathogen, in this AD model. Most patients with asthma have elevated serum IgE levels and concomitant atopic eczema and allergic rhinitis. *Aspergillus* species are strong fungal allergens²⁷. We believe that our AD model and MSC-Ex treatment mimic the atopic conditions and the treatment thereof in a clinical setting, and MSC-Ex could provide an alternative therapeutic tool for AD.

Materials and Methods

Ethics statement. This work was approved by the Institutional Review Board of Asan Medical Center (authorization no. 2015-0303). The research was conducted in accordance with Helsinki Declaration. All of the participating women provided written informed consent. All animal experiments were performed in accordance with relevant guidelines and regulations of the Animal Ethics Committee of Asan Medical Center (authorization no. 2015-12-220) accredited for laboratory animal care by Ministry of Food and Drug Safety of South Korea.

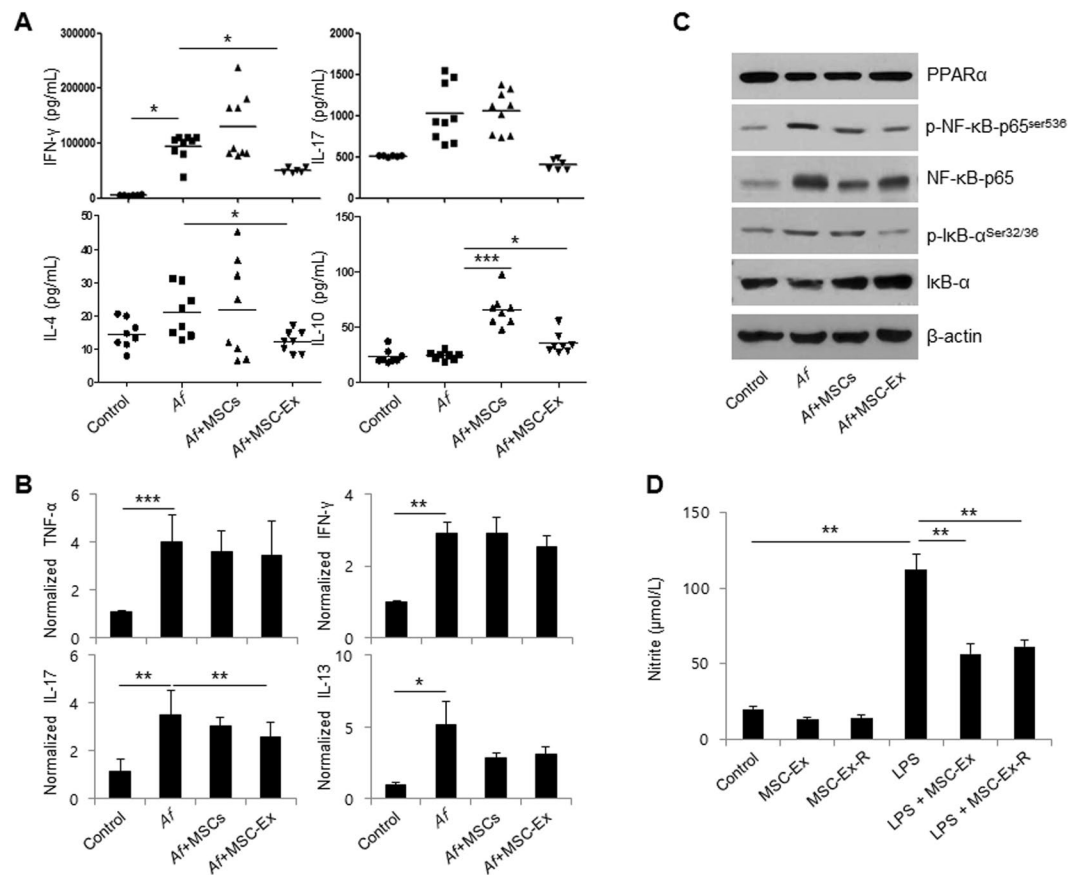


Figure 5. MSC-Ex downregulates LN-derived Th1, Th2 and Th17 cell activation. (A) IFN- γ , IL-17, IL-4 and IL-10 levels in anti-CD3/CD28 stimulated lymphocytes from the LNs of Af-treated mice were measured by ELISA. Data are represented as the means \pm s.d. ($n \geq 6$ mice per group). (B) The relative expression levels of the inflammatory-associated cytokines, TNF- α , IFN- γ , IL-17 and IL-13, were evaluated by qRT-PCR in the skin tissues of AD mice. (C) The protein levels of PPAR α , p-NF- κ B-p65^{Ser536}, NF- κ B-65, p-I κ B^{Ser32/36} and I κ B, were analyzed by immunoblotting in the skin tissue of AD mice. (D) The levels of nitrite were measured using the culture media from the basolateral side of MSC-Ex and RAW 264.7 co-cultures after 4 h of LPS (1 μ g/ml) treatment and subsequent MSC-Ex (30 μ g/ml) administration for 24 h. Columns represent the means of three independent experiments. Bars indicate standard deviations. * $P < 0.05$, ** $P < 0.005$, *** $P < 0.001$.

Cell culture and treatment. HaCaT (human keratinocyte) cells were maintained in DMEM (Invitrogen-Gibco, Carlsbad, CA) containing 10% fetal bovine serum, penicillin (100 U/ml), and streptomycin (100 g/ml) (Invitrogen-Gibco) at 37 °C in a humidified 5% CO₂ incubator. HaCaT cells were pretreated with bacterial LPS (*E. coli*, serotype 055:B5, 100 μ g/ml; Sigma-Aldrich, St. Louis, MO) for 4 h or TNF- α (300-01 A; PEPROTECH, Rocky Hill, NJ) and IFN- γ (300-02; PEPROTECH) (10 ng/ml each) for 2 h and then treated with MSC-Ex (30 μ g/ml) in the presence of LPS or TNF- α /IFN- γ for an additional 24 h. RAW264.7 cells were incubated with LPS (1 μ g/ml) for 4 h. After incubation, the RAW264.7 cells were washed three times in ice-cold UC-MSCs were washed twice with cold phosphate-buffered saline (PBS), and treated with MSC-Ex (30 μ g/ml) for 24 h.

Isolation and expansion of UC-MSCs. UC-MSCs were prepared as previously described¹⁵. Briefly, after removing the vessels and amnion, Wharton's jelly tissues were minced and digested for 3 h in MEM (11095-080; Invitrogen-Gibco) with 0.1% collagenase A (10103578001; Roche, Mannheim, Germany) at 37 °C in a shaking incubator. They were then filtered through a 70 μ m mesh (103760; BD Falcon, San Jose, CA) and pelleted using low-speed centrifugation at 200 \times g for 10 min. The isolated cells were cultured in DMEM supplemented with 10% FBS. MSCs at passages 3–5 were pooled for subsequent MSC-Ex or MSC therapies. UC-MSCs were characterized with a panel of surface markers (positive for CD29, CD73, CD90 and CD105 and negative for CD34 and CD45) (Supplementary Fig. S1).

Preparation of MSC-Ex. UC-MSCs were washed twice with cold PBS and resuspended in five times the packed cell volume of PBS. After 30 min of incubation on dry ice, the cells were transferred to a water bath maintained at 37 °C for 3 min. The cells then underwent two cycles of freezing and thawing. After centrifugation at 12,000 \times g for 10 min, the supernatant was collected and stored at -80 °C. For lyophilization, frozen

MSC-Ex samples were transferred to a lyophilizer (Alpha 1–4 LSC plus Entry Freeze Dryer; John Morris Group, Queensland, Australia) operating at -55°C and 0.0715 mbar. The frozen lysates were dried for ~24 h and reconstituted in PBS.

Quantitative real-time reverse transcription-polymerase chain reaction (qRT-PCR). Total RNA was isolated using the FavorPrep Total RNA Mini Kit (FABRK001; Vienna, Austria). First-strand cDNA was synthesized from 1 μg of total RNA using the SuperScriptTMII enzyme (18064-014; Invitrogen). qRT-PCR was performed on an Applied Biosystems 7900HT Fast Real-Time PCR System using the Power SYBR Green PCR Master Mix (326759; Warrington, UK) with the following primers: GAPDH, GAAGGTGAAGGTCCGAGTC (forward) and GAAGATGGTATGGGATTTTC (reverse); IL-6, AATTCGGTACATCCTCGACGG (forward) and GGTGTTTTCTGCCAGTGCC (reverse); IL-1 β , AAAAGCTTGGTATGTCTGG (forward) and TTTCAACACGCAGGACAGG (reverse); TNF- α , GGAGAAGGGTGACCGACTCA (forward) and CTGCCAGACTCGGCAA (reverse); IL-4, CCGTAACAGACATCTTTGCTGCC (forward) and GAGTGCCTTCTCATGGTGGCT (reverse); IL-5, GGAATAGGCACACTGGAGAGTC (forward) and CTCTCCGTCTTCTTCTCCACAC (reverse); iNOS, TCAGCCAAGCCCTCACCTAC (forward) and CCAATCTCTGCCTATCCGTCTC (reverse); IL-10, GATCCAGTTTACCTGGAGGAG (forward) and CCTGAGGGTCTTCAGGTTCTC (reverse); TGF- β 1, CACCCGCGTGC TAATGG (forward) and TGTGTACTCTGCTTGAATCTGTCAT (reverse); m β -actin, GGCTGTATCCCTCCATCG (forward) and CCAGTTGGTAACAATGCCATGT (reverse); mTNF- α , AACTCCAGGCGGTGCC TATG (forward) and TCCAGTCTCCTCCACTTG (reverse); mIFN- γ , TCAAGTGGCATAGATGTGGAAGAA (forward) and TGGCTCTGCAGGATTTTCATG (reverse); mIL-17, CAGGGAGAGCTTCATCTGTGT (forward) and GCTGAGCTTTGAGGGATGAT (reverse); mIL-13, GCAGCATGGTATGGAGTGTG (forward) and TGGCGAAACAGTTGCTTTGT (reverse). The amplification protocol consisted of an initial denaturation step at 95°C for 5 min, then 35 cycles at 94°C for 15 s, 60°C for 15 s, and 72°C for 15 s, followed by a final extension step at 72°C for 10 min. The expression level of the above genes was normalized to that of GAPDH.

Western blot analysis. Whole-cell lysates were prepared in cell lysis buffer (Cell Signaling Technology, Beverly, MA, USA) containing a protease inhibitor cocktail (Tech & InnovationTM, Bucheon, Korea) and a phosphatase inhibitor cocktail (sc-45065; Santa Cruz Biotechnology, Santa Cruz, CA). Proteins were then separated on an SDS-PAGE gel and analyzed with the following primary antibodies: PPAR α (ac24509; Abcam, Cambridge, MA), p-NF- κ B (ab86299; Abcam), NF- κ B (sc-372; Santa Cruz Biotechnology), p-I κ B- α (sc-101713; Santa Cruz), I κ B (sc-371; Santa Cruz), iNOS (PA1-036; Thermo Scientific, Rockford, IL), and β -actin (A5441; Sigma-Aldrich).

***Aspergillus fumigatus* (Af)-induced AD model.** BALB/c 8 weeks mice were purchased from Orient Bio Inc. (Seongnam, South Korea). The mice were anesthetized with 60 mg/kg of Zoletil 50[®] (Virbac, Laboratories, Carros, France), and their dorsal hair was shaved with clippers. 40 μg of *Aspergillus fumigatus* (Af) extract (XPM3D3A25; Greer Laboratories, Lenoir, NC, USA) was then epicutaneously applied to a 1 cm² area on the dorsal surface for 5 days. The procedure was repeated twice at 2 week intervals. Control mice were treated similarly with the same amount of PBS alone. The mice ($n \geq 6$ animals per group) were then subcutaneously injected with either MSCs (2×10^6 cells/mouse) or MSC-Ex (300 μg /mouse) on day 23 after commencing the Af treatment.

Clinical symptom scoring and epidermal permeability barrier function assessment. The severity of dermatitis was assessed weekly using the following scoring procedure: 0, no symptoms; 1, mild; 2, moderate; and 3, severe. These scores were applied to itching, edema, hemorrhage, excoriation/erosion, and scaling/dryness, expressed as the sum of the scores for these five symptoms (maximum score, 15)²⁸. The epidermal permeability barrier function was evaluated by transepidermal water loss (TEWL) measurements with a Vapometer[®]SWL-3 (Delfin Technologies Ltd., Kuopio, Finland) at the same site and on the same day as the clinical score determination.

Lymph node cultures. Skin lymph nodes (LNs) were dissected immediately after sacrifice and kept on ice in RPMI-1640 media (Gibco) with 10% fetal bovine serum and 1% penicillin/streptomycin (Gibco). Cell suspensions were obtained by pressing the LNs through a cell strainer (40 μm) (SPL Life science, Pocheon, South Korea) and seeded at 4×10^6 cells/well. LN cells were cultured in the presence of CD3 (3 $\mu\text{g}/\text{mL}$) and CD28 (1 $\mu\text{g}/\text{mL}$) antibodies at 37°C for 2 days and their supernatants were collected and quantitatively analyzed for mIFN- γ (88-7314-22; Invitrogen), and mIL-17 (88-7371-22; Invitrogen), mIL-4 (KET7007; Abbkine, Wuhan, China) and mIL-10 (900K53EK; PEPROTECH) by enzyme-linked immunosorbent assay (ELISA).

Total serum immunoglobulin E (IgE) measurement. Blood samples were obtained from the inferior vena cava of the mice immediately after sacrifice. Serum was separated from the blood clots by centrifugation at 2,000 rpm for 10 minutes at 20°C and stored at -80°C . Total serum immunoglobulin E (IgE) concentrations were measured by ELISA (#555248; BD).

Histological evaluation. Dermatitis severity was assessed microscopically in the mice as indicated in Supplementary Table 1 using the following scoring system: skin sections of the dorsal surface were stained with hematoxylin and eosin (H&E) and graded for inflammation (0, none; 1, mild; 2, moderate; 3, severe), depth of fibrosis (0, none; 1, ~0.3 mm; 2, ~0.5 mm; 3, ~0.8 mm; 4, ~1 mm), parakeratosis and/or hyperkeratosis (0, none; 1, reduced; 2, no change), hypergranulosis (0, none; 1, reduced; 2, no change) and psoriasiform epidermal hyperplasia (0, none; 1, reduced; 2, no change). The score for each parameter was multiplied by a factor reflecting the percentage of tissue involvement to yield the final score.

Statistical analysis. All data are expressed as the mean \pm s.d. Statistical significance was evaluated using the non-parametric Wilcoxon rank sum test and defined as $P < 0.05$.

References

1. Odhiambo, J. A. *et al.* Global variations in prevalence of eczema symptoms in children from ISAAC Phase Three. *J Allergy Clin Immunol* **124**, 1251–1258, <https://doi.org/10.1016/j.jaci.2009.10.009> (2009).
2. Silverberg, J. I. & Hanifin, J. M. Adult eczema prevalence and associations with asthma and other health and demographic factors: a US population-based study. *J Allergy Clin Immunol* **132**, 1132–1138, <https://doi.org/10.1016/j.jaci.2013.08.031> (2013).
3. Schneider, L., Tilles, S., Lio, P., Boguniewicz, M. & Beck, L. Atopic dermatitis: a practice parameter update 2012. *J Allergy Clin Immunol* **131**, 295–299, <https://doi.org/10.1016/j.jaci.2012.12.672> (2013).
4. Simon, D., Braathen, L. R. & Simon, H. U. Eosinophils and atopic dermatitis. *Allergy* **59**, 561–570, <https://doi.org/10.1111/j.1398-9995.2004.00476.x> (2004).
5. Uccelli, A., Pistoia, V. & Moretta, L. Mesenchymal stem cells: a new strategy for immunosuppression? *Trends Immunol* **28**, 219–226, <https://doi.org/10.1016/j.it.2007.03.001> (2007).
6. He, A., Feldman, S. R. & Fleischer, A. B. Trends in Atopic Dermatitis Management: Comparison of 1990–1997 to 2003–2012. *J Drugs Dermatol* **17**, 135–140 (2018).
7. Misery, L. Therapeutic perspectives in atopic dermatitis. *Clin Rev Allergy Immunol* **41**, 267–271, <https://doi.org/10.1007/s12016-010-8226-y> (2011).
8. Berke, R., Singh, A. & Guralnick, M. Atopic dermatitis: an overview. *Am Fam Physician* **86**, 35–42 (2012).
9. Eichenfield, L. F. *et al.* Guidelines of care for the management of atopic dermatitis: section 2. Management and treatment of atopic dermatitis with topical therapies. *J Am Acad Dermatol* **71**, 116–132, <https://doi.org/10.1016/j.jaad.2014.03.023> (2014).
10. Shin, T. H. *et al.* Human adipose tissue-derived mesenchymal stem cells alleviate atopic dermatitis via regulation of B lymphocyte maturation. *Oncotarget* **8**, 512–522, <https://doi.org/10.18632/oncotarget.13473> (2017).
11. Kim, H. S. *et al.* Clinical Trial of Human Umbilical Cord Blood-Derived Stem Cells for the Treatment of Moderate-to-Severe Atopic Dermatitis: Phase I/IIa Studies. *Stem Cells* **35**, 248–255, <https://doi.org/10.1002/stem.2401> (2017).
12. Troyer, D. L. & Weiss, M. L. Wharton's jelly-derived cells are a primitive stromal cell population. *Stem cells* **26**, 591–599, <https://doi.org/10.1634/stemcells.2007-0439> (2008).
13. Seshareddy, K., Troyer, D. & Weiss, M. L. Method to isolate mesenchymal-like cells from Wharton's Jelly of umbilical cord. *Methods Cell Biol* **86**, 101–119, [https://doi.org/10.1016/S0091-679X\(08\)00006-X](https://doi.org/10.1016/S0091-679X(08)00006-X) (2008).
14. Singer, N. G. & Caplan, A. I. Mesenchymal stem cells: mechanisms of inflammation. *Annu Rev Pathol* **6**, 457–478, <https://doi.org/10.1146/annurev-pathol-011110-130230> (2011).
15. Song, J. Y. *et al.* Umbilical cord-derived mesenchymal stem cell extracts reduce colitis in mice by re-polarizing intestinal macrophages. *Sci Rep* **7**, 9412, <https://doi.org/10.1038/s41598-017-09827-5> (2017).
16. Kim, D. W. *et al.* Wharton's jelly-derived mesenchymal stem cells: phenotypic characterization and optimizing their therapeutic potential for clinical applications. *Int J Mol Sci* **14**, 11692–11712, <https://doi.org/10.3390/ijms140611692> (2013).
17. Karp, J. M. & Leng Teo, G. S. Mesenchymal stem cell homing: the devil is in the details. *Cell Stem Cell* **4**, 206–216, <https://doi.org/10.1016/j.stem.2009.02.001> (2009).
18. Yang, L. *et al.* Oleylethanolamide exerts anti-inflammatory effects on LPS-induced THP-1 cells by enhancing PPAR α signaling and inhibiting the NF- κ B and ERK1/2/AP-1/STAT3 pathways. *Sci Rep* **6**, 34611, <https://doi.org/10.1038/srep34611> (2016).
19. Zhang, N. *et al.* Peroxisome proliferator activated receptor alpha inhibits hepatocarcinogenesis through mediating NF- κ B signaling pathway. *Oncotarget* **5**, 8330–8340, <https://doi.org/10.18632/oncotarget.2212> (2014).
20. Moudgil, K. D. Interplay among cytokines and T cell subsets in the progression and control of immune-mediated diseases. *Cytokine* **74**, 1–4, <https://doi.org/10.1016/j.cyto.2015.05.006> (2015).
21. Kamota, T. *et al.* Ischemic pre-conditioning enhances the mobilization and recruitment of bone marrow stem cells to protect against ischemia/reperfusion injury in the late phase. *J Am Coll Cardiol* **53**, 1814–1822, <https://doi.org/10.1016/j.jacc.2009.02.015> (2009).
22. Kay, A. G. *et al.* Mesenchymal Stem Cell-Conditioned Medium Reduces Disease Severity and Immune Responses in Inflammatory Arthritis. *Sci Rep* **7**, 18019, <https://doi.org/10.1038/s41598-017-18144-w> (2017).
23. Krampera, M. Mesenchymal stromal cell 'licensing': a multistep process. *Leukemia* **25**, 1408–1414, <https://doi.org/10.1038/leu.2011> (2011).
24. Polchert, D. *et al.* IFN- γ activation of mesenchymal stem cells for treatment and prevention of graft versus host disease. *Eur J Immunol* **38**, 1745–1755, <https://doi.org/10.1002/eji.200738129> (2008).
25. Romieu-Mourez, R. *et al.* Cytokine modulation of TLR expression and activation in mesenchymal stromal cells leads to a proinflammatory phenotype. *J Immunol* **182**, 7963–7973, <https://doi.org/10.4049/jimmunol.0803864> (2009).
26. Koga, C. *et al.* Possible pathogenic role of Th17 cells for atopic dermatitis. *J Invest Dermatol* **128**, 2625–2630, <https://doi.org/10.1038/jid.2008.111> (2008).
27. Agarwal, R. *et al.* Severe asthma and fungi: current evidence. *Med Mycol* **49**(Suppl 1), S150–157, <https://doi.org/10.3109/13693786.2010.504752> (2010).
28. Akei, H. S. *et al.* Epicutaneous aeroallergen exposure induces systemic TH2 immunity that predisposes to allergic nasal responses. *J Allergy Clin Immunol* **118**, 62–69, <https://doi.org/10.1016/j.jaci.2006.04.046> (2006).

Acknowledgements

This work was supported by grants from the Korea Health Technology R&D Project through the Korea Health Industry Development Institute (KHIDI), Ministry of Health, Welfare and Family Affairs, Republic of Korea (HI15C2111), from the National Research Foundation of Korea (NRF-2017R1A2B4002758), and from the Asan Institute for Life Sciences, Asan Medical Center, Seoul, Korea (W16-644).

Author Contributions

Ji-young Song, acquisition of data; Hyo Jeong Kang, review of pathology; Hyun Min Ju, acquisition of data; Arum Park, technical support; Hyojung Park, technical support; Joon Seok Hong, obtainment of study materials; Chong Jai Kim, analysis and interpretation of data; Jae-Yoon Shim, obtainment of study materials; Jinho Yu, conceived and designed the study; Jene Choi, supervised the study, obtaining funding and wrote the manuscript.

Additional Information

Supplementary information accompanies this paper at <https://doi.org/10.1038/s41598-019-42964-7>.

Competing Interests: The authors declare no competing interests.

Publisher's note: Springer Nature remains neutral with regard to jurisdictional claims in published maps and institutional affiliations.



Open Access This article is licensed under a Creative Commons Attribution 4.0 International License, which permits use, sharing, adaptation, distribution and reproduction in any medium or format, as long as you give appropriate credit to the original author(s) and the source, provide a link to the Creative Commons license, and indicate if changes were made. The images or other third party material in this article are included in the article's Creative Commons license, unless indicated otherwise in a credit line to the material. If material is not included in the article's Creative Commons license and your intended use is not permitted by statutory regulation or exceeds the permitted use, you will need to obtain permission directly from the copyright holder. To view a copy of this license, visit <http://creativecommons.org/licenses/by/4.0/>.

© The Author(s) 2019